Applied Physics B (2019) 125:105
https://doi.org/10.1007/s00340-019-7218-8

Applied Physics B
Lasers and Optics

Nonlinear manipulation of circular Airy beams

Qichang Jiang[1] · Yanli Su[1] · Ziwei Ma[1] · Yonghong Li[1] · Wei Zheng[1]

Received: 30 December 2018 / Accepted: 13 May 2019 / Published online: 20 May 2019

Abstract
We investigate the propagation property of circular Airy beams in photorefractive nonlinear media by differential method. The abruptly autofocusing behavior of circular Airy beams in free space is first discussed. The intensity contrast will increase with the decreasing of decay factor and the focal length will also increase with the increasing of initial radius. When photorefractive nonlinearity is introduced, the energy diffusion of circular Airy beams after autofocusing behavior can be manipulated. The periodic breather soliton can be obtained when the energy diffusion is suppressed by appropriately photorefractive nonlinearity. If the photorefractive nonlinearity is large enough, the abruptly autofocusing behavior is suppressed completely and the circular Airy beam can form the bracelet breather soliton.

1 Introduction

Abruptly autofocusing (AAF) beams possess a ring-shaped initial transverse Airy intensity profile, which maximum intensity remain almost constant during propagation until they propagate a certain distance and show AAF behavior [1–3]. Due to this novel property, AAF beams are ideal candidates for laser biomedical treatment, microparticle manipulation, multiphoton polymerization, and high-power terahertz generation [4–7]. Circular Airy (CAi) beams are the first AAF beams to be proposed. Recent researches have shown that the propagation trajectory as well as position of autofocusing points of the CAi beam can be manipulated by a dynamic linear potential, and the different types of dynamic linear potentials can weaken or strengthen the autofocusing effect of the CAi beam [8–10]. Moreover, the CAi beam can exhibit periodic AAF behavior under the action of radial parabolic potentials, and form a series of elegant periodic optical bottles having paraboloidal shapes [11]. More recently, more generalized Airy beams with AAF behavior, such as Airyprime beams [12], fractional Airy beams [13], azimuthally modulated circular superlinear Airy (AMCSAi) beams [14] and circular superlinear chirp (CSC) beams [15], have been reported. In contrast to the traditional CAi beam, the AMCSAi beam does not focus on a point on the axis due to the petal patterns. The CSC beam provides faster and more abrupt focusing than the traditional CAi beam.

At the same time, the propagation properties of the one- or two-dimensional Airy and generalized Airy beams in the nonlinear medium have been widely reported [16–25]. They found that the self-acceleration effect of the Airy beam can be weakened by the nonlinearity and the breather can be obtained under appropriately nonlinear conditions. People naturally think how the nonlinearity of media influences the propagation property of the CAi beam. In this article, we will investigate the propagation property of the CAi beam in photorefractive nonlinear media.

2 Theoretical model

Given that a CAi beam propagating in strontium barium niobate crystals (SBN), the propagation dynamics of the CAi beam is described by the following equation [9, 22]:

$$i\frac{\partial\phi}{\partial z}+\frac{1}{2}\left(\frac{\partial^2\phi}{\partial x^2}+\frac{\partial^2\phi}{\partial y^2}\right)-\beta\frac{\phi}{1+|\phi|^2}=0, \tag{1}$$

✉ Qichang Jiang
jiangsir009@163.com

Yanli Su
syli1979@163.com

Ziwei Ma
twlz168@tom.com

Yonghong Li
liyonghong02721227@163.com

Wei Zheng
zhengweinku@163.com

[1] Department of Physics and Electronic Engineering, Yuncheng University, Yuncheng 044000, China

where ϕ is the beam envelope, x and y are the normalized transverse coordinates scaled by transverse width x_0, z is the propagation distance scaled by Rayleigh length kx_0^2, and $k = (2\pi/\lambda_0)n_e$. λ_0 is the free space wavelength, and n_e is the unperturbed extraordinary index of refraction. $\beta = (2\pi x_0/\lambda_0)^2(n_e^4 r_{33}/2)E_0$ is the photorefractive nonlinearity parameter, r_{33} is the electro-optic coefficient, and E_0 is the external electric field. We take transverse width $x_0 = 100\ \mu$m, $\lambda_0 = 532$ nm, $n_e = 2.35$, $r_{33} = 224 \times 10^{-12}$ m/V, and the Rayleigh length is about 277.4 mm.

The intensity profile of the inward CAi beam at the input plane can be expressed as:

$$\phi\,(x, y) = \mathrm{A}_0 \mathrm{Ai}\,(r_0 - r)\ \exp[\alpha\,(r_0 - r)], \tag{2}$$

where A_0 is a constant, Ai is the Airy function, r_0 is the initial radius of the main Airy ring, $r = \sqrt{x^2 + y^2}$ is the radial distance, and α is the decay factor.

3 Propagation property of the CAi beam

In this section, we analyze the propagation property of the CAi beam by solving numerically Eq. (1). First, the intensity profiles and propagation properties of the CAi beam in free space are analyzed as shown in Fig. 1. The intensity contrast M is defined as the ratio of the peak intensity along the propagation to the peak intensity at the input place, which depicts the focusability of the CAi beam. The value of M is higher, the focusability is higher. The propagation distance z at the maximum intensity contrast represents the focus position and the value of z is the focal length of the CAi beam. Only the section drawing when $y = 0$ is given because of the symmetrical intensity distribution.

In the following, we focus on the manipulation of focusability. We can find that the intensity contrast M increases with the decreasing of the decay factor α while the focal length is nearly constant as shown in Fig. 2. Moreover, the focal length increases with the increasing of the initial radius r_0 while the intensity contrast M has changed little as shown in Fig. 3. For the AMCSAi beam, the focal length decreases with the increasing of the power order, i.e., the degree of

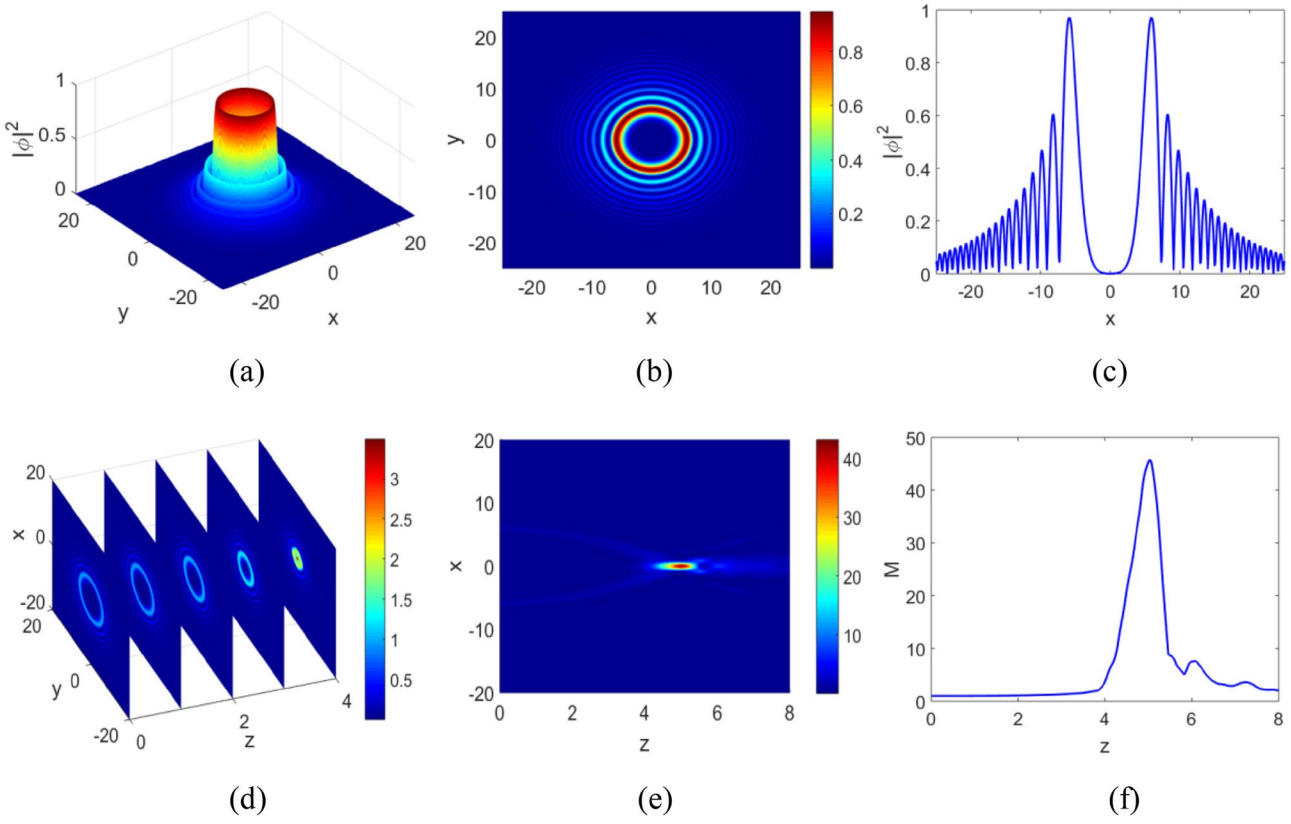

Fig. 1 The intensity profiles and propagation properties of the CAi beam when $A_0 = 2$, $r_0 = 5$, and $\alpha = 0.1$. **a**–**c** are the space drawing, projection drawing, and section drawing, respectively. **d** is the propagation property in free space. **e** is the section drawing of the propagation when $y = 0$. **f** is the intensity contrast M under different propagation distance z

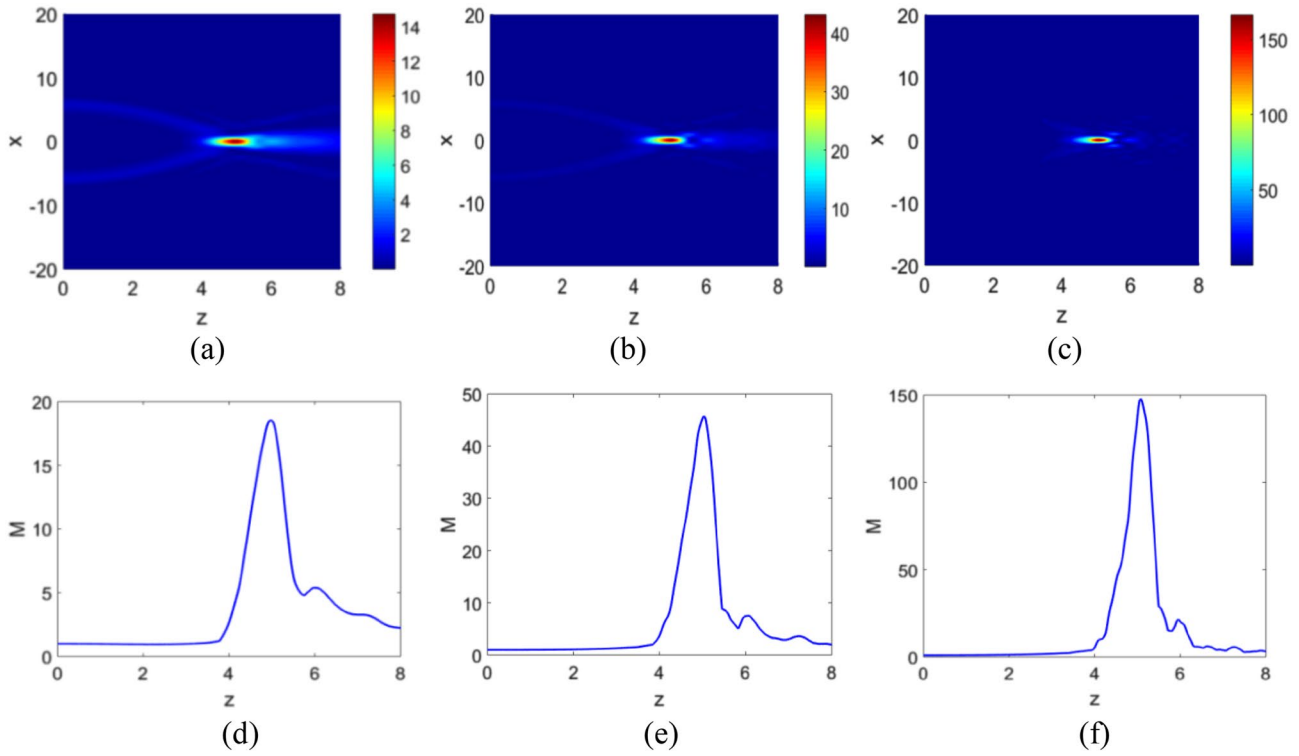

Fig. 2 The relation between the focusability of the CAi beam and the decay factor α when $A_0 = 2$, $r_0 = 5$. **a**–**c** are the section drawing when decay factor $\alpha = 0.2$, $\alpha = 0.1$, and $\alpha = 0.01$, respectively. **d**–**f** are the corresponding intensity contrast

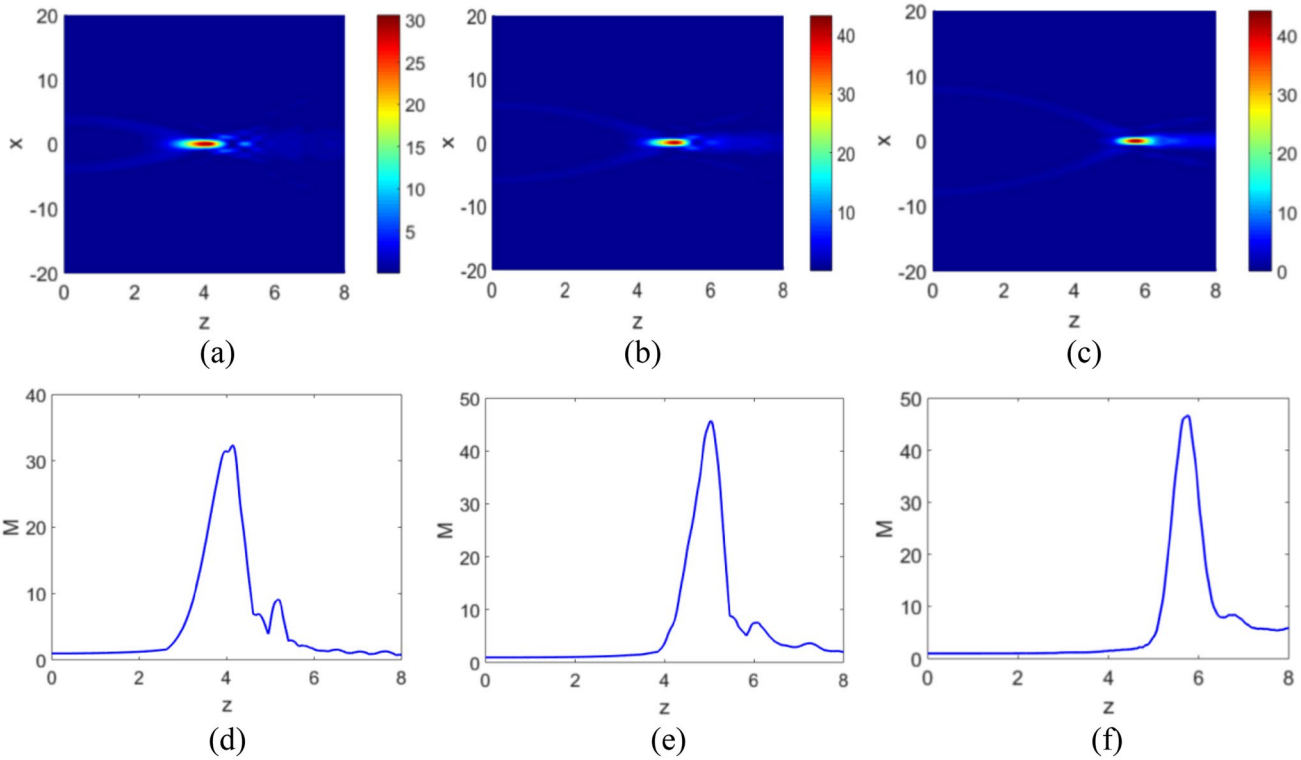

Fig. 3 The relation between the focusability of the CAi beam and the initial radius r_0 of the main Airy ring when $A_0 = 2$, $\alpha = 0.1$. **a**–**c** are the section drawing when initial radius $r_0 = 3$, $r_0 = 5$, and $r_0 = 8$, respectively. **d**–**f** are the corresponding intensity contrast

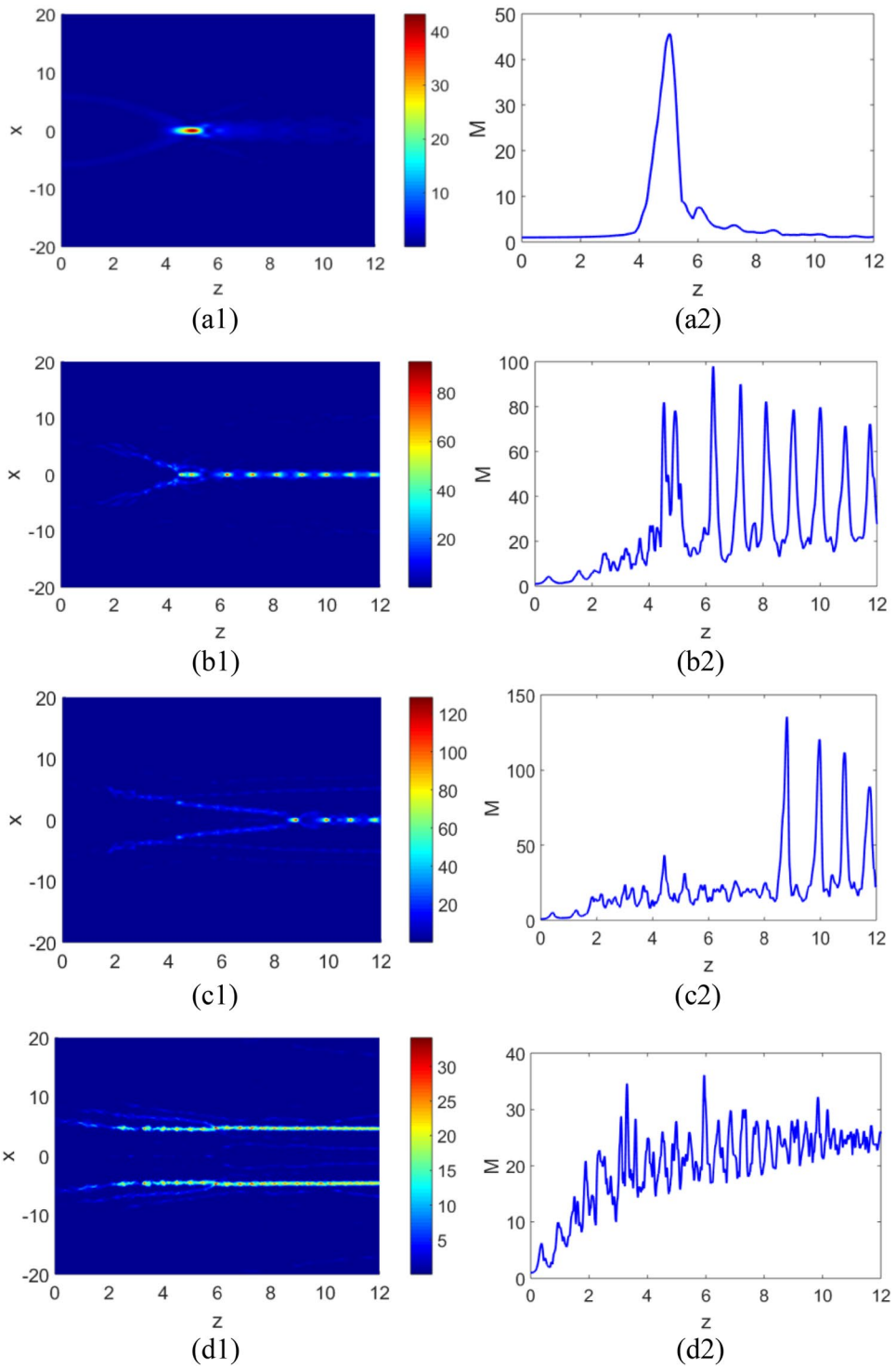

Fig. 4 The nonlinear manipulation of the CAi beam when $A_0 = 2$, $r_0 = 5$, and $\alpha = 0.1$. **a1**–**d1** are the section drawing when nonlinear parameter $\beta = 0$, $\beta = 20$, $\beta = 26$, and $\beta = 35$, respectively. **a2**–**d2** are the corresponding intensity contrast

nonlinearity of the radius [14] and for the CSC beam, the focal length decreases with the increasing of the power order and chirp order [15].

Next, we investigate the propagation property of the CAi beam in photorefractive media, and analyze the impact of photorefractive nonlinearity on the AAF behavior of the CAi beam. When the photorefractive nonlinearity parameter $\beta = 0$, we can find that the positon of autofocusing points is about $z = 5$, and the intensity contrast is about $M = 45$. If the photorefractive nonlinearity is introduced, the energy diffusion of the CAi beam after the focus point is manipulated. The CAi beam will form the breather soliton with periodic focusing behavior when the photorefractive nonlinearity parameter β be increased from 0 to 20. At the

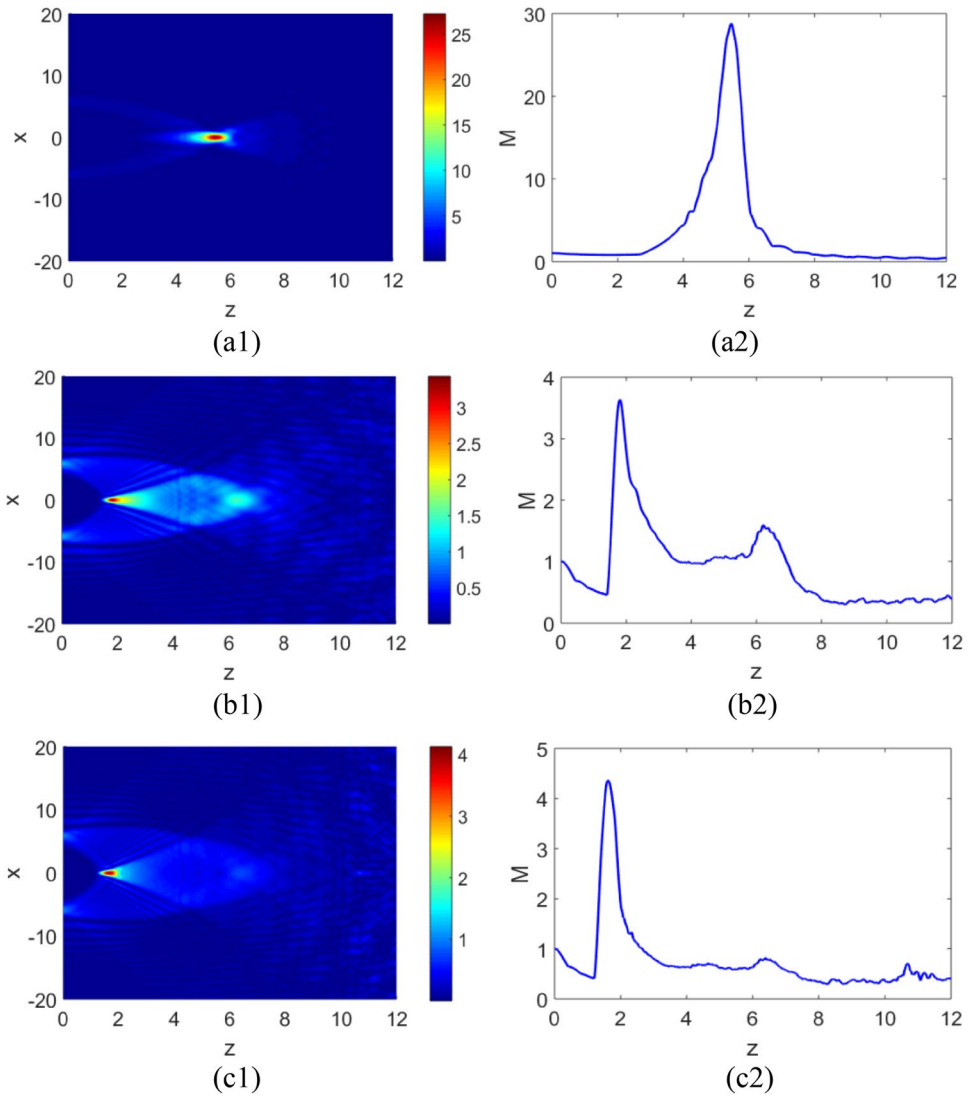

Fig. 5 The nonlinear manipulation of the CAi beam when the self-defocusing nonlinearity is introduced and $A_0 = 2$, $r_0 = 5$, and $\alpha = 0.1$. **a1**–**c1** are the section drawing when nonlinear parameter $\beta = -2$, $\beta = -10$, and $\beta = -15$, respectively. **a2**–**c2** are the corresponding intensity contrast

same time, the first focus position almost unchanged but the peak value at the focus improves greatly to about $M = 80$ as shown in Fig. 4b. As the increasing continuously of the photorefractive nonlinearity, the AAF behavior is suppressed corresponding to the focal length increases. When the photorefractive nonlinearity is large enough, such as $\beta = 35$, the AAF behavior of the CAi beam is suppressed completely and the bracelet breather soliton can be obtained as shown in Fig. 4d.

Finally, we discuss the manipulation property of the CAi beam when the nonlinearity parameter is negative. We can find that the focal length and the intensity contrast both decrease when the self-defocusing nonlinearity is introduced as shown in Fig. 5. We think the reason for this is that the self-defocusing nonlinearity accelerates the energy diffusion of the CAi beam and leads to the significant shift of the focus to the input plane.

4 Conclusions

In summary, we have investigated the influence of photorefractive nonlinearity on the propagation property of the CAi beam. The focal length and intensity contrast both can be manipulated by varying nonlinear parameter. After the focus point, the CAi beam can form periodic breather soliton when the energy diffusion is suppressed by appropriately photorefractive nonlinearity and then the bracelet breather soliton also can be obtained when the AAF behavior is suppressed completely by photorefractive nonlinearity.

Acknowledgements This work was supported by the Natural Science Foundation of Shanxi Province, China (Grant no. 201801D121023) and the Doctor Scientific Research Fund of Yuncheng University (Grant no. YQ-2018004).

References

1. N.K. Efremidis, D.N. Christodoulides, Opt. Lett. **35**, 4045 (2010)
2. D.G. Papazoglou, N.K. Efremidis, D.N. Christodoulides, S. Tzortzakis, Opt. Lett. **36**, 1842 (2011)
3. I. Chremmos, N.K. Efremidis, D.N. Christodoulides, Opt. Lett. **36**, 1890 (2011)
4. P. Zhang, J. Prakash, Z. Zhang, M.S. Mills, N.K. Efremidis, D.N. Christodoulides, Z.G. Chen, Opt. Lett. **36**, 2883 (2011)
5. Y.Q. Zhang, H. Zhong, M.R. Belic, Y.P. Zhang, Appl. Sci. **7**, 341 (2017)
6. M. Manousidaki, D.G. Papazoglou, M. Farsari, S. Tzortzakis, Optica **3**, 525 (2016)
7. K. Liu, A.D. Koulouklidis, D.G. Papazoglou, S. Tzortzakis, X.C. Zhang, Optica **3**, 605 (2016)
8. C.Y. Hwang, K.Y. Kim, B. Lee, IEEE Photonics J. **4**, 174 (2012)
9. H. Zhong, Y.Q. Zhang, M.R. Belic, C.B. Li, F. Wen, Z.Y. Zhang, Y.P. Zhang, Opt. Express **24**, 7495 (2016)
10. X.W. Long, J. Bai, Optik **165**, 356 (2018)
11. J.G. Zhang, X.S. Yang, Opt. Commun. **420**, 163 (2018)
12. G.Q. Zhou, R.P. Chen, G.Y. Ru, Laser Phys. Lett. **12**, 025003 (2015)
13. S.N. Khonina, A.V. Ustinov, J. Opt. Soc. Am. A **34**, 1991 (2017)
14. A.P. Porfirev, S.N. Khonina, J. Opt. Soc. Am. B **34**, 2544 (2017)
15. S.N. Khonina, A.P. Porfirev, A.V. Ustinov, J. Opt. **20**, 025605 (2018)
16. S. Jia, J. Lee, J.W. Fleischer, G.A. Siviloglou, D.N. Christodoulides, Phys. Rev. Lett. **104**, 253904 (2010)
17. R.P. Chen, C.F. Yin, X.X. Chu, H. Wang, Phys. Rev. A **82**, 043832 (2010)
18. I. Dolev, I. Kaminer, A. Shapira, M. Segev, A. Arie, Phys. Rev. Lett. **108**, 113903 (2012)
19. Y.Q. Zhang, M.R. Belic, H.B. Zheng, H.X. Chen, C.B. Li, Y.Y. Li, Y.P. Zhang, Opt. Express **22**, 7160 (2014)
20. T. Bouchet, N. Marsal, M. Sciamanna, D. Wolfersberger, Phys. Rev. A **97**, 051801(R) (2018)
21. C.D. Chen, B. Chen, X. Peng, D.M. Deng, J. Opt. **17**, 035504 (2015)
22. B. Liu, K.Y. Zhan, Z.D. Yang, J. Opt. Soc. Am. B **35**, 2794 (2018)
23. Q.C. Jiang, Y.L. Su, H.X. Nie, Z.W. Ma, Y.H. Li, Appl. Phys. B **124**, 36 (2018)
24. J.B. Zhang, K.Z. Zhou, J.H. Liang, Z.Y. Lai, X.L. Yang, D.M. Deng, Opt. Express **26**, 1290 (2018)
25. Q.C. Jiang, Y.L. Su, Z.W. Ma, W. Zheng, Y.H. Li, H.X. Nie, J. Mod. Opt. **65**, 2243 (2018)